Pergamon

Bioorganic & Medicinal Chemistry 8 (2000) 1423–1432

BIOORGANIC & MEDICINAL CHEMISTRY

Antimycobacterial Pyrroles: Synthesis, Anti-*Mycobacterium tuberculosis* Activity and QSAR Studies

Rino Ragno,[a] Garland R. Marshall,[a,*] Roberto Di Santo,[b] Roberta Costi,[b] Silvio Massa,[c] Raffaello Rompei[d] and Marino Artico[b,*]

[a]*Center for Molecular Design, Washington University, St. Louis, MO 63110, USA*
[b]*Dipartimento di Studi Farmaceutici, Università degli Studi di Roma "La Sapienza", P. le A. Moro 5, 00185 Rome, Italy*
[c]*Dipartimento Farmaco Chimico Tecnologico, Università degli Studi di Siena, Banchi di Sotto 55, 53100 Siena, Italy*
[d]*Cattedra di Microbiologia Applicata, Facoltà di Scienze Matematiche, Fisiche e Naturali, Università di Cagliari, via Porcel 4, 09124 Cagliari, Italy*

Received 10 November 1999; accepted 17 February 2000

Abstract—A number of known antifungal pyrrole derivatives and some newly synthesized compounds (**5**–**33**) were tested in vitro against *Mycobacterium tuberculosis* CIP 103471. The majority of tested compounds were efficient antimycobacterial agents showing MIC values ranging from 0.5 to 32 μg/mL. A 3-D-QSAR study has been performed on these pyrrole derivatives to correlate their chemical structures with their observed inhibiting activity against *M. tuberculosis*. Due to the absence of information on a putative receptor responsible for this activity, classical quantitative structure–activity relationships (QSAR) and comparative molecular field analysis (CoMFA) have been applied. A model able to well correlate the antimycobacterial activity with the chemical structures of pyrrole derivatives **5**–**33** has been developed which is potentially helpful in the design of novel and more potent antituberculosis agents. The combination of CoMFA with classical QSAR descriptors led to a better hybrid 3-D-QSAR model, that successfully explains the structure–activity relationships ($r^2 = 0.86$) of the training set. A comparison between the QSAR, CoMFA and mixed QSAR–CoMFA models is also presented. The hybrid model is to be preferred, however, because of its lowest values of the average absolute error of prediction toward a limited external test set.

Introduction

The search for novel antibacterial agents active against *Mycobacterium tuberculosis* and other atypical mycobacteria is urgent due to the lack of effectiveness of known antituberculosis agents against opportunistic pathogens as a consequence of rapidly emerging resistance. Furthermore, immunocompromised patients observed with AIDS, or after transplantation, are easily infected by pathogenic fungi, protozoa and mycobacteria, leading rapidly to death. In particular, mycobacteria have recently increased their virulence and about 30 million of people are predicted by the World Health Organization (WHO) to catch tuberculosis in the near future.[1–5] Despite the efforts of the pharmaceutical companies engaged in the design, synthesis and assays of new potent and selective antituberculosis agents, the current therapeutic outlook is poor. Only a few derivatives were found endowed with some antimycobacterial activity, including Upjohn oxazolidinone **1** (U-100480),[6,7] the nitroimidazo[2,1-*b*]oxazole **2**,[8,9] some broad-spectrum esters of pyrazinoic acid **3**[10] and 5-chloropyrazinamide **4**[11] (Chart 1). While the mechanisms of action of clinical antituberculosis agents have been intensively investigated, the details of their interaction with their target enzymes are not known.[12,13]

Recently, pyrrole derivatives have emerged as chemotherapeutic agents potentially useful for inhibiting the activities of *M. tuberculosis* and other atypical mycobacteria, including *M. avium* complex, an opportunistic pathogen that greatly contributes to the death of AIDS patients. Porretta and co-workers[14] have reported the antimycobacterial activity of a pyrrole derivative, and Di Santo et al.[15] more recently ascribed appreciable inhibiting action to pyrrolnitrin and some related nitropyrroles **5**–**12** and **19**–**23**.

*Corresponding authors. Garland R. Marshall: Tel.: +1-314-362-1567; fax: +1-314-362-0234; garland@gpc.wust.l.edu; Marino Artico: Tel./fax: +39-6-446-2731; artico@uniroma1.it.

0968-0896/00/$ - see front matter
PII: S0968-0896(00)00061-4

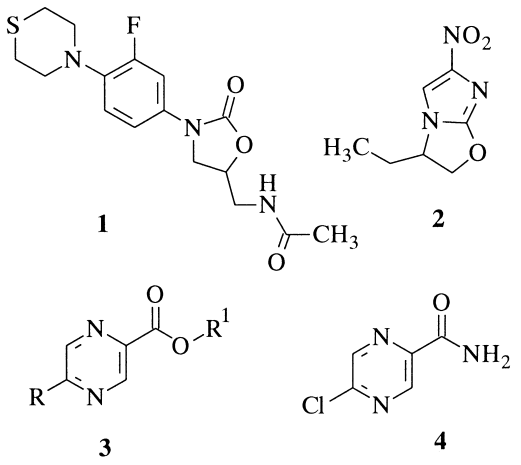

Chart 1.

Keeping in mind the above results, we tested against *M. tuberculosis* a number of pyrrole derivatives (**5**–**12**, **19**–**24** and **31**–**33**)[15–18] and some newly synthesized compounds (**13**–**18** and **25**–**30**) related to the above pyrroles (Table 1), in which the phenyl moiety was replaced by a pyridine ring typical of isoniazid (INH), which is nowadays the most potent antituberculosis agent in clinical practice.

With the aim of establishing the role of the pyrrole ring as a pharmacophoric group and, hence, its influence on the antimycobacterial activity, we have undertaken a 3-D-QSAR study on this set of pyrrole derivatives. Since no information regarding their putative receptor is available, classical quantitative structure–activity relationships (QSAR) and comparative molecular field analysis (CoMFA)[19–21] were used to correlate the antimycobacterial activity of compounds **5**–**33** (Table 1) showing some level of inhibitory potency (Tables 2 and 3) against *M. tuberculosis*.

Table 1. Pyrrole derivatives used for training set and test set

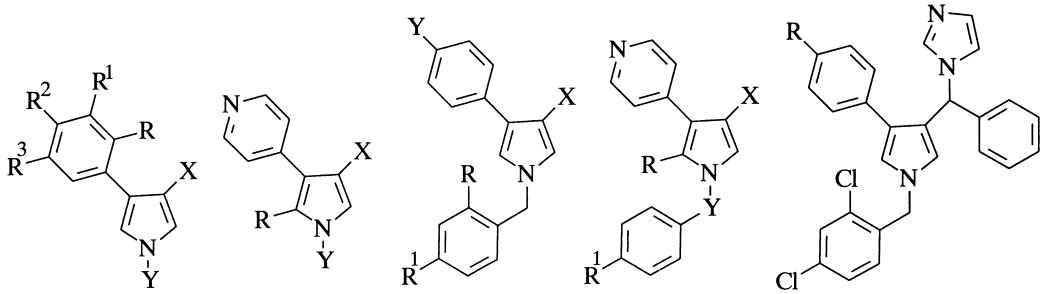

5–12 **13–18** **19–24** **25–30** **31–33**

Compd	X	Y	R	R^1	R^2	R^3	MIC[a] (μg/mL)	Reference
5	COOEt	H	H	H	Cl	H	16	15,16
6	NO_2	H	Cl	H	Cl	H	1	15,17
7[b]	NO_2	H	Cl	Cl	H	H	16	15,17
8	NO_2	H	H	Cl	Cl	H	8	15,17
9	NO_2	H	H	Cl	H	Cl	8	15,17
10	NO_2	H	Cl	H	OH	H	32	17
11[b]	NO_2	CH_3	Cl	H	OCH_3	H	>250	15,17
12	COOEt	CH_3	H	H	OCH_3	H	16	15,16
13	COOEt	H	H	—	—	—	16	—
14	$CONHNH_2$	H	H	—	—	—	>250	—
15	COOEt	CH_3	H	—	—	—	16	—
16	COOEt	C_2H_5	H	—	—	—	16	—
17	COOEt	H	C_2H_5	—	—	—	250	—
18	$CONHNH_2$	H	C_2H_5	—	—	—	>250	—
19	COOH	Cl	H	Cl	—	—	16	15,16
20	COOEt	OCH_3	H	H	—	—	8	15,16
21	COOEt	OCH_3	H	F	—	—	16	15,16
22[b]	COOEt	H	H	F	—	—	125	15,16
23	CH_2OH	H	Cl	H	—	—	8	15
24[b]	$CH(OH)C_6H_5$	H	Cl	Cl	—	—	250	18
25	COOEt	CH_2	H	Cl	—	—	0.50	—
26	COOEt	CH_2	C_2H_5	H	—	—	4	—
27	$CONHNH_2$	CH_2	H	Cl	—	—	16	—
28	COOEt	SO_2	H	CH_3	—	—	4	—
29[b]	COOEt	SO_2	H	NO_2	—	—	>250	—
30	CH_2OH	SO_2	H	CH_3	—	—	4	—
31	—	—	H	—	—	—	16	18
32	—	—	F	—	—	—	1	18
33[b]	—	—	OCH_3	—	—	—	1	18

[a]Minimum inhibiting concentration of test derivatives against *Mycobacterium tuberculosis* CIP 103471. Reference drugs: INH (MIC = 0.2 μg/mL) and SM (MIC = 0.7 μg/mL). The assays were done in triplicate. The degree of variation was found always within 50%.
[b]Used for test set.

Table 2. Training set: QSAR parameters and recalculated pMICs

Compd	Exp pMIC	HlogP	DipMom	LUMO	Vol	G_CDS	Fitted pMIC		
							COMFA	Mixed	QSAR
5	4.19	4.49	5.50	0.17	217.41	−2.66	4.21	4.20	4.16
6	5.41	4.10	7.50	−0.65	191.88	−4.72	5.37	5.44	5.37
8	4.51	4.10	4.79	−0.65	192.69	−5.01	4.53	4.51	4.49
9	4.51	4.10	5.76	−0.67	192.42	−5.11	4.57	4.81	4.80
10	3.87	2.84	5.76	−0.67	186.43	−8.86	3.86	4.12	4.14
12	4.21	3.77	4.89	0.52	245.67	−0.32	4.17	3.72	3.60
13	4.13	2.45	6.14	0.18	197.49	−4.08	4.12	3.82	3.78
14	2.61	0.06	6.29	0.25	179.61	−9.72	2.51	2.59	2.68
15	4.16	2.39	6.60	0.22	215.03	−1.39	4.28	4.16	4.07
16	4.18	2.93	6.95	0.24	231.40	−1.01	4.16	4.26	4.28
17	2.99	3.53	6.06	0.39	232.08	−3.00	3.05	3.76	3.82
18	2.66	1.26	6.27	0.39	213.33	−8.72	2.56	2.72	2.82
19	4.34	5.44	4.44	−0.49	285.72	−3.09	4.26	4.44	4.46
20	4.62	5.32	5.06	−0.06	318.64	0.58	4.58	4.49	4.46
21	4.34	5.34	4.53	−0.37	322.29	0.82	4.46	4.52	4.61
23	4.62	4.83	5.20	−0.35	284.59	−2.91	4.53	4.48	4.43
25	5.83	4.53	7.90	−0.53	301.98	−1.44	5.49	5.48	5.47
26	4.92	5.02	6.76	−0.09	321.83	−0.14	4.95	4.90	4.87
27	4.31	2.26	6.74	−0.42	283.50	−6.68	4.67	4.00	3.98
28	4.97	4.27	3.09	−1.01	320.64	−2.93	4.41	4.13	4.15
30	4.91	2.43	5.29	−1.58	284.11	−6.05	5.00	4.74	4.76
31	4.46	5.60	6.03	−0.66	401.27	0.99	5.00	5.15	5.20
32	5.68	5.55	6.54	−0.71	404.80	1.73	5.13	5.40	5.45

Table 3. Test set: actual and residual pMICs

Compd	Experimental	CoMFA model		Mixed model		QSAR model	
		Pred.	Residual	Pred.	Residual	Pred.	Residual
7	4.21	4.43	−0.22	5.06	−0.85	4.01	−1.21
11	2.73	4.14	−1.41	3.85	−1.12	3.80	−1.07
22	3.41	5.19	−1.78	4.41	−1.00	4.42	−1.01
24	3.21	4.24	−1.03	3.69	−0.48	4.01	−0.80
29	2.90	4.31	−1.41	4.31	−1.41	4.44	−1.54
33	5.69	4.85	0.84	4.57	1.12	4.62	1.07

Chemistry

Derivatives used for this study have been prepared either according to procedures described in previous works[15–18] or by the pathway depicted in Scheme 1.

Condensation of pyridine-4-carboxaldehyde with triethylphosphonoacetate in the presence of anhydrous K_2CO_3 furnished 3-(4-pyridinyl)-2-propenoic acid ethyl ester,[22] that was annulated with the proper toluene-4-sulfonylalkyl isocyanide[23] in the presence of sodium hydride to give pyrroles **13** and **17**. Potassium salt of **13** reacted with arylsulfonyl chlorides in the presence of 18-crown-6 as a catalyst to obtain sulfones **28** and **29** and lithium aluminum hydride reduction of the latter compound furnished the related carbinol **30**.

Alkylation of pyrroles **13** and **17** with formation of derivatives **15**, **16**, **25** and **26** was performed by phase transfer catalysis using tetrabutylammonium hydrogen sulfate and the proper alkyl halide in a mixture of dichloromethane and concentrated aqueous NaOH. Finally, treatment of esters **13**, **17** and **25** with hydrazine hydrate in boiling ethanol gave carboxyhydrazides **14**, **18** and **27**, respectively.

Molecular Modeling and QSAR Methods

All the computational work was performed on Silicon Graphics computers (Indigo2 R10000 195 MHz and Octane 225 MHz). The measurements of biological activity used to develop the QSAR and the CoMFA were expressed as (pMIC) = −log(MIC), where MIC is the minimal inhibiting concentration expressed as molar concentration (Tables 2 and 3). To the four derivatives which have been found to be 'inactive' (MIC > 250 μg/mL) an activity value equal to 50% of that of the compound reported as the less active was arbitrarily assigned. Although such data might contribute to a disturbing source of noise, it is, nevertheless, true that the exclusion of a non-negligible number of observations would imply serious loss of information.[24,25]

For systems in which no information exists about the binding site, it is a well established assumption to consider that a similar class of molecules (congeneric series) binds to the putative receptor site adopting a similar geometry and orientation. Since structural overlap is the simplest hypothesis, we decided to test its self-consistency before deriving a more complicated model. For this reason, no particular effort was made to explore the

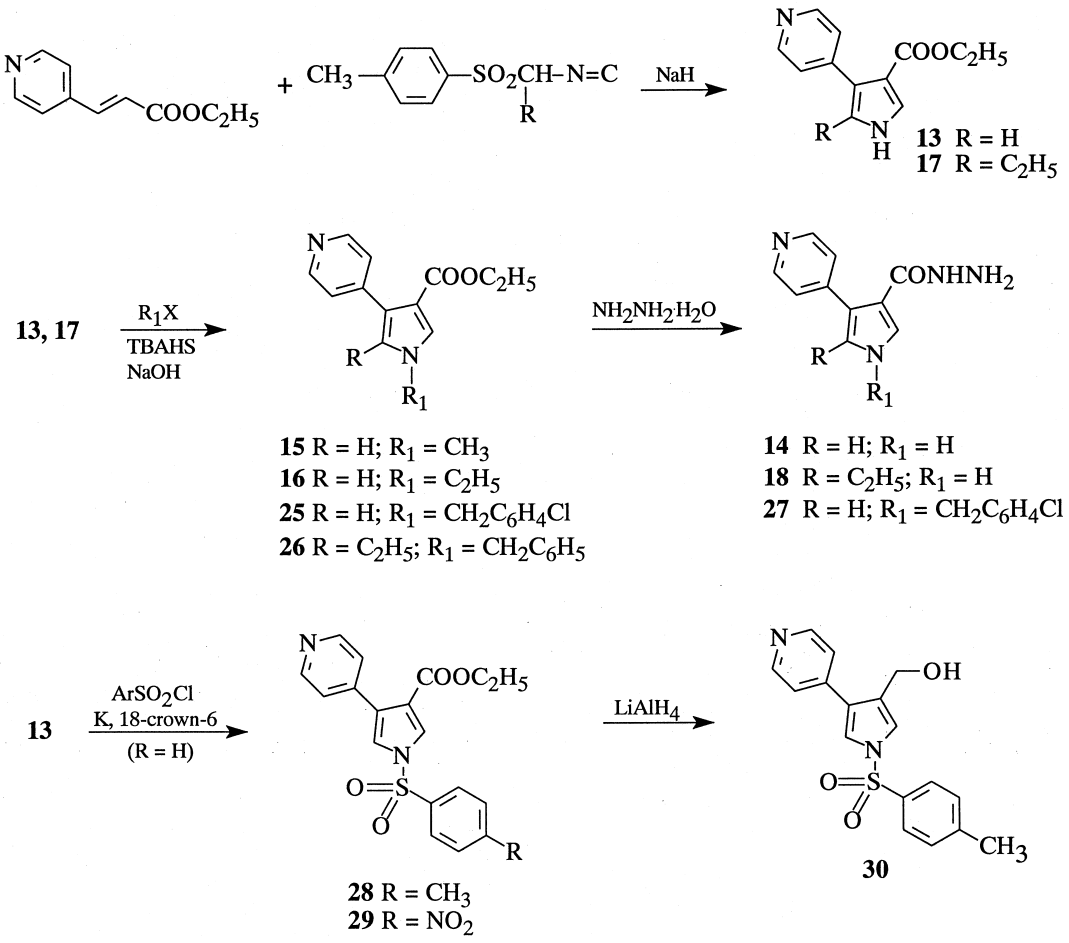

Scheme 1.

conformational space of the tested molecules to seek alternative binding modes. A goal of future work will be to determine possible binding geometries that define a common pharmacophoric pattern and generate a 3-D receptor model.

All the molecules were built using the SKETCH module implemented in the program SYBYL[26] starting from the lowest energy conformation of the searched template molecule (**32**). Before any alignment trial, the geometry of each molecule was optimized by a simple minimization to the nearest local minimum using the MMFF94[27] force field implemented in SYBYL.

CoMFA calculations were performed with the QSAR module of SYBYL and the following parameters. The grid in which the aligned molecules were embedded was regularly spaced (2 Å) with dimensions of 22×22×16 Å, the same region used to align the molecules by the field-fitting techniques. A further refinement of the region was done with the PLS region focusing[28] option in the QSAR-SYBYL module. Region focusing is an iterative procedure that refines a model by increasing the weight for those lattice points that are most pertinent to the model. Steric and electrostatic interaction energies were calculated using a carbon sp^3 probe with a +1 charge, a distance-dependent dielectric constant ($1/r$), and an energetic cutoff of 30 kcal/mol with no electrostatic interactions at sterically bad contacts. For both the CoMFA fields and the field-fit alignment, the atomic point charges were obtained from a semiempirical calculation using the AM1 hamiltonian implemented in MOPAC93. Regression analyses were done using the SYBYL implementation of the PLS algorithm, initially with leave-one-out (LOO) cross-validation to reduce the possibility of obtaining chance correlations and eight principal components (PCs).[29]

The optimal number of PCs was then chosen on the basis of the highest cross-validated q^2 value, the smallest standard error of prediction (SEP), and the minimum number of components. To improve the signal-to-noise ratio, the minimum sigma value was set to 2.0 kcal/mol. The steric and electrostatic field columns were weighted according to the CoMFA-STD default scaling option, where a field is considered as a whole and every CoMFA variable is affected by the overall field mean and standard deviation. Final PLS with no cross-validation was then carried out using the optimal number of PCs.

Along with the standard CoMFA fields, the influences of some classical QSAR parameters were also taken into account. Several parameters were computed for each

molecule and added to the CoMFA analysis spreadsheet: (i) the program HINT[30] version 2.25 was used to estimate the logarithm of the partition coefficient (HlogP);[31] (ii) from MOPAC93 (1SCF calculation, AM1 hamiltonian) the HOMO and LUMO energies;[32] (iii) the ionization potential and the dipole moment; (iv) from the AMSOL (1SCF calculation, AM1 hamiltonian) program the molecular volume (Vol) along with the cavity dispersion energies were obtained (G-CDS, G-P and G-P-CDS).[32]

Results and Discussion

Antimycobacterial activity

Pyrrole derivatives **5**–**33** were assayed in vitro against *M. tuberculosis* CIP 103471 and their activities are reported in Table 1 together with those of INH and streptomycin (SM) used as reference drugs. Most test derivatives inhibited the growth of *M. tuberculosis* at MIC values ranging from 0.5 to 250 μg/mL. In particular, compound **25** showed the highest potency (0.5 μg/mL) comparable to reference drugs, while four derivatives, namely **11**, **14**, **18** and **28**, were devoid of any antituberculosis activity. Imidazoles **32**–**33** and nitropyrrole **6** showed MIC = 1 μg/mL, similar to that of streptomycin, while compounds **26**, **28** and **30** were 4 times less potent. The remaining derivatives showed interesting MIC values (8–32 μg/mL) with the exception of the slightly active pyrroles **17**, **22** and **24** (MIC = 125–250 μg/mL).

Molecular modeling and QSAR

The calculated QSAR parameters were correlated with the in vitro measured inhibitory activities of the synthesized compounds. The molecular data set was split in a training set of 23 molecules and a test set of 6 molecules (Tables 2 and 3). The splitting was based on two principal concepts: (1) an activity range ($\Delta pMIC_{TrainingSet}$ = 2.61–5.83; $\Delta pMIC_{TestSet}$ = 2.73–5.69) of the two sets as close as possible and (2) the maximum chemical diversity of the test set.

In developing a CoMFA model, the alignment of the training set is the most important step. Because no structural information existed on the nature of the receptor and, hence, of the binding site, the field-fit procedure was used to align the training set. Compound **32** was used as template molecule on the basis of being both one of the more sterically constrained as well as one of the more active. The random search module implemented in SYBYL was used to select the conformation of the template molecule. The MMFF94 force field with the default settings was used. The lowest energy conformation obtained was then used to build all the other molecules of the training and test sets. A field-fit alignment with subsequent minimization was carried out twice to obtain the final alignment used in the analysis. As the compounds belong to a congeneric series, the particular conformation chosen is not expected to have a significant effect on the statistical quality of the CoMFA model derived. The cross-validation analysis using only the CoMFA fields led to a model with an optimal number of principal components (PCs) of 4, a q^2 value of 0.44 and a standard error of prediction (SEP) of 0.78 log units. The corresponding non-cross-validated analysis (4 PCs) resulted in a fitted r^2 value of 0.933 (Fig. 1), with a standard error of estimation (SEE) of 0.229 (F-test value = 62.729) (CoMFA MODEL). The contributions of the steric and electrostatic fields were, respectively, 50.5 and 49.5%. The model did not show very good predictive statistical results (q^2 only 0.44) but was still valuable, since it was shown that CoMFA models showing a q^2 higher than 0.3 have a low probability of chance correlation.[29] The low value of q^2 may be due to some deficiencies in the molecular alignment, but several attempts to improve the CoMFA model varying the alignment did not lead to better results; for instance, the more obvious atom by atom alignment based on the common skeleton atoms led to a CoMFA model with almost the same statistical characteristics, but slightly worse than that obtained by the field-fit alignment.

The combination of the previous CoMFA with classical QSAR descriptors led to a better 3-D-QSAR model. After several trials, the best relationship was obtained by including the HINT calculated logP (HlogP), the dipole moment (DipMom), the LUMO energy, the molecular volume (Vol) and the cavity-dispersion-solvent structure free energy (G_CDS). The optimal number of PCs for this hybrid model was found to be 3, for which a q^2 value of 0.73 was obtained with a SEP of 0.45 pMIC units. With 3 PCs, a r^2 value of 0.86 was obtained (HYBRID MODEL), with a SEE of 0.32 units (Fig. 2).

In contrast with classical QSARs, it is not possible to write a regression equation for CoMFA 3-D-QSAR models because of the large number of variables. On the other hand, the CoMFA model has the advantage that the 3-D correlated results can be graphically displayed.

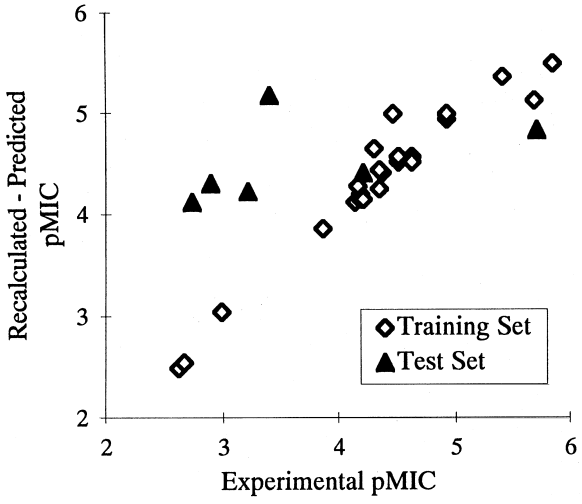

Figure 1. CoMFA model: training set fitting and test set predictions.

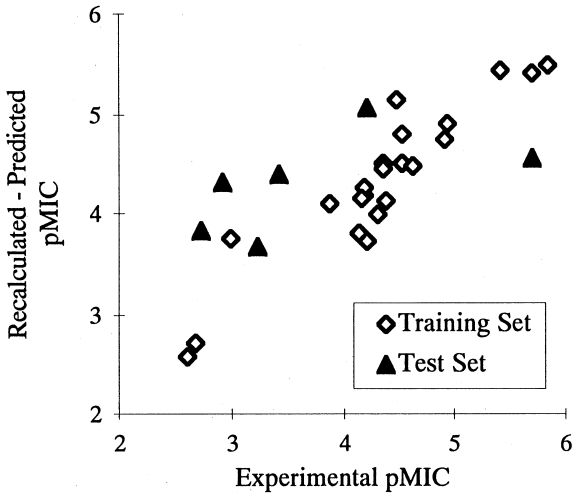

Figure 2. Hybrid model: training set fitting and test set predictions.

The CoMFA steric and electrostatic field contour maps give information about those regions where a modification of the chemical structure can enhance, or decrease, the biological activity. The surfaces are the representation of those lattice points, where differences in field values are correlated with differences in activity. In Figure 3 are shown the maps for the CoMFA and the mixed models, that are coincident, where the red contours represent regions of decreased tolerance for positive charge (20% contribution), the blue contours represent regions of decreased tolerance for negative charge (80% contribution), the yellow contours represent regions of low steric tolerance (20% contribution) and the green contours represent regions of high steric tolerance (80% contribution).

The interpretation of these maps is highly subjective; the absence of lattice points does not mean that a given pharmacophoric element has no influence on the biological activity, but only that almost all the compounds included in the training set exert similar steric and/or electrostatic influence in that particular area, or, alternatively, that the lack of polyhedra in some regions delineates a less explored space.

As can be seen in Figure 3, large green polyhedra run around the aromatic moiety directly attached to the pyrrole indicating a good correlation of the activity with the presence of bulky substituents on the 2-aryl portion. Yellow polyhedra situated around the space where the ethyl group of the carboxyethyl substituent is present in almost all the molecules indicate a decreasing activity induced with the presence of some bulky group in that position. However, due to the flexible nature of the ethyl moiety and because the molecules after the field fitting were minimized it is not possible to make any assumptions regarding this particular portion of the space. A rather important blue spot is visible around the region where the lone pair of the carboxyl oxygen is located. Since the presence of a lone pair donating atom is almost always present, we can assume that for some level of activity a hydrogen bonding donor in that region is required. Finally two large red polyhedra are located where the sulfonyl moiety exists for some compounds included in the training set. In this case we assume that the conformations used represent the binding geometry, and the red polyhedra represent a region of the putative binding site where a hydrogen bond could occur.

Because of the high contribution to the final QSAR analysis, a PLS analysis was also carried out using only the QSAR descriptors, giving a q^2 of 0.70 and a standard error of prediction (SEP) value of 0.46 pMIC units

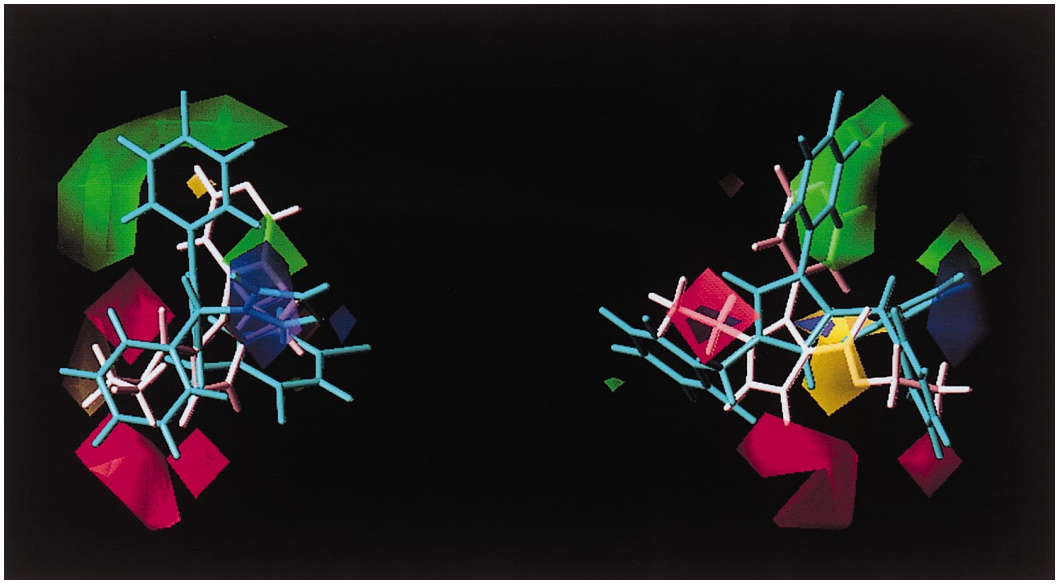

Figure 3. CoMFA electrostatic and steric STDEV*COEFF contours plot from the analysis CoMFA and Mixed. Negative charge not favorite areas (contribution level 80%) are represented by the red polyhedra. Negative charge-favored areas (contribution level 20%) are represented by blue polyhedra. Sterically favored areas (contribution level 80%) are represented by green polyhedra. Sterically unfavored areas (contribution level 20%) are represented by yellow polyhedra. Along with the contours are displayed also two molecules, one active in cyan **32** and one less active in white **17**.

using 3 PCs (Fig. 4). The non-cross-validated PLS resulted in a conventional correlation coefficient (r^2) value of 0.83 (QSAR MODEL) and a standard error of estimation (SEE) of 0.36 log unit (F-test value = 30.0). Here is the QSAR regression equation obtained using only the traditional QSAR parameters:

$$\begin{aligned} \text{pMIC} = & 2.437 + (0.245)^{*}\text{HlogP} + (0.313) \\ & {}^{*}\text{DipMom} - (0.969)^{*}\text{LUMO} - (0.003) \\ & {}^{*}\text{Vol} + (0.097)^{*}\text{G\_CDS} \end{aligned}$$

From the regression equation, it is possible to observe that there is a strong correlation between the parameters and the biological activity. Since all parameters used are global descriptors of the molecule as a whole, it is not possible to relate specific molecular structural differences to the contribution of each variable and little molecular design insight is obtained.

In general, a modification leading to an increase of the overall lipophilicity should lead to an increase of activity (high positive coefficients for HlogP and G_CDS). On the other hand, the overall bulk of the molecules does not have to increase too much (small negative coefficient for the molecular volume) to decrease activity. In respect to the other two important parameters, LUMO and DipMom, they seem to be in agreement with what was observed for the previous CoMFA maps. Large variations of the electrostatic nature of the molecule may lead to large variations of the biological activity (high coefficients for both the dipole moment and the LUMO energy of opposite sign).

A set of six compounds reserved from training was used to test the efficacy of the obtained models. The models show almost the same statistical coefficients, although the best overall is the mixed QSAR–CoMFA model showing the lowest value of both the average absolute error of prediction (1.00) and SDEP (1.04). All the models show moderate overprediction as can be seen from Figures 1, 2 and 4, where the experimental biological activities are plotted versus the predicted activities. In almost all the cases, the models tend to predict a greater value for this limited test set.

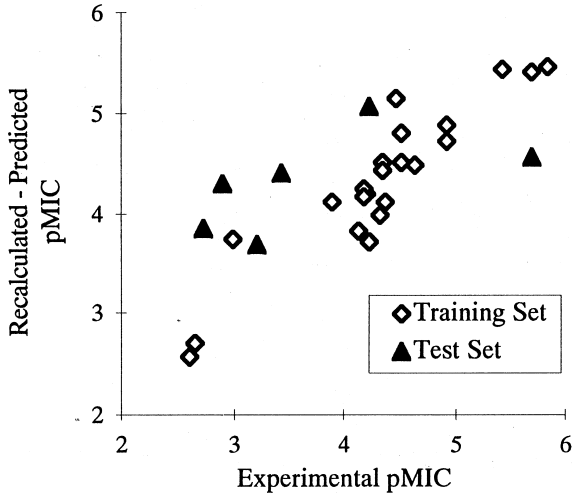

Figure 4. Hybrid model: training set fitting and test set predictions.

Conclusions

We have described the synthesis, antimicrobial activity and QSAR studies of pyrrole derivatives endowed with anti-*M. tuberculosis* activity. A number of these compounds showed good potency in in vitro assays and pyrrole **25** resulted as active as SM and two and half times less potent than INH used as reference drugs. This compound will be considered as lead for further investigations on antimycobacterial pyrrole derivatives.

A variation of the CoMFA method with the inclusion of some classical QSAR descriptors has led to the definition of a hybrid QSAR–CoMFA model that successfully explains the structure–activity relationships ($r^2 = 0.86$) of the training set. Considering the limited range of pMIC (ΔpMIC = 3) we did not expect to obtain an excellent predictive QSAR model but only to find out some relationship to be used in the design of more potent compounds. When we applied an external test set the HYBRID MODEL was capable of discriminating between the more and less active compounds showing reasonable error of prediction (SDEP = 1.04). Such a value of SDEP could also be obtained if one used the average of the training set as a predictor but in this case no trend is obtained. Moreover from the associated graphical CoMFA contour maps it is possible to derive some suggestions to modify our lead compound and design new potential antimycobacterial agents. In particular the large green polyhedra around the aromatic moiety in position 4 of pyrrole ring suggests the introduction of a small lipophilic substituent that could increase the antimycobacterial activity. In fact, considering the obtained classical QSAR equation, a higher value of logP and G_CDS along with a limited enhancement of the molecular volume could lead to more potent derivatives. Moreover the CoMFA maps suggest the introduction of more molecular diversity to explore those regions that were not found relevant in the 3-D-QSAR.

Experimental

Melting points were determined on a Büchi 530 melting point apparatus and are uncorrected. Infrared (IR) spectra (Nujol mulls) were recorded on a Perkin–Elmer 297 instrument. ^{1}H NMR spectra were recorded at 200 MHz on a Bruker AC 200 spectrometer. Chemical shifts are reported in δ (ppm) units relative to the internal reference tetramethylsilane (TMS). All compounds were routinely checked by TLC and ^{1}H NMR. TLC was performed by using Stratocrom SIF Fluka (silica gel precoated plates with fluorescent indicator) or Stratocrom ALF Fluka (aluminum oxide precoated plates

with fluorescent indicator). Developed plates were visualized by UV light. Chromatographic purifications were performed on Merck aluminum oxide (70–230 mesh) and Merck silica gel (70–230 mesh). Solvents were reagent grade and, when necessary, were purified and dried by standard methods. Concentration of solutions after reactions and extractions involved the use of a rotary evaporator operating at a reduced pressure of approximately 20 Torr. Organic solutions were dried over anhydrous sodium sulfate. Analytical results agreed to within ± 0.40% of the theoretical values. Microanalyses were performed by Laboratories of Dipartimento di Scienze Farmaceutiche, Università di Padova, Italy. Chemical and physical data of newly synthesized compounds **13**–**18** and **25**–**30** are reported in Table 4.

Syntheses

Specific examples presented below illustrate general synthetic procedures.

Ethyl 3-(4-pyridinyl)-2-propenoate. A solution of pyridine-4-carboxaldehyde (5.0 g, 0.047 mol) in absolute ethanol (80 mL) was added into a well stirred mixture of triethylphosphonoacetate (12.6 g, 0.056 mol) and anhydrous potassium carbonate (19.5 g, 0.141 mol). The resulting suspension was stirred at 70 °C for 2.5 h, then the solvent was removed and the residue was treated with water (300 mL) and extracted with chloroform (3×150 mL). The organic extracts were collected, washed with brine (3×200 mL) and dried. Evaporation of the solvent gave pure ethyl 3-(4-pyridinyl)-2-propenoate (8.33 g, 100% yield).[22]

Ethyl 5-ethyl-4-(4-pyridinyl)pyrrole-3-carboxylate (17). A solution of ethyl 3-(4-pyridinyl)-2-propenoate (3.0 g, 0.017 mol) and 1-(4-methylphenylsulfonyl)propylisocyanide[23] (3.8 g, 0.017 mol) in anhydrous dimethylsulfoxide:diethyl ether (30:60 mL) mixture was added by dropping into a well-stirred suspension of sodium hydride (0.068 mol, 2.7 g of 60% suspension in white oil) in anhydrous diethyl ether (80 mL) under argon stream. When addition stopped the mixture was stirred at room temperature for 15 min, treated with water (200 mL) and extracted with ethyl acetate (3×100 mL). The organic extracts were collected, washed with brine (3×200 mL) and dried. Removal of the solvent gave a crude product which was chromatographed on aluminum oxide column (ethyl acetate as eluent) to give pure **17** (1.5 g, 36% yield); IR: ν 2700 (NH) and 1680 (CO) cm^{-1}; ^1H NMR ($CDCl_3$): δ 1.18 (m, 6H, CH_3), 2.58 (q, 2H, CH_2CH_3), 4.16 (q, 2H, OCH_2CH_3), 7.27 (m, 2H, pyridine C3-H and C5-H), 7.43 (d, 1H, $J_{1,2}=3.0$ Hz, pyrrole C2-H), 8.57 (m, 2H, pyridine C2-H and C6-H), 9.10 (bs, 1H, NH); anal. $C_{14}H_{16}N_2O_2$ (244.29) C, H, N.

This procedure was used for the synthesis of **13** starting from toluene-4-sulfonylmethylisocyanide (TosMIC). Spectroscopic data of **13** are reported below.

13: IR: ν 3100 (NH) and 1710 (CO) cm^{-1}; ^1H NMR (DMSO-d_6): δ 1.21 (t, 3H, CH_3), 4.15 (q, 2H, CH_2), 7.19 (m, 1H, pyrrole C5-H), 7.47–7.56 (m, 3H, pyridine C3-H and C5-H and pyrrole C2-H), 8.47 (m, 2H, pyridine C2-H and C6-H), 11.77 (bs, 1H, NH); anal. $C_{12}H_{12}N_2O_2$ (216.24) C, H, N.

Ethyl 1-(4-nitrobenzenesulfonyl)-4-(4-pyridinyl)pyrrole-3-carboxylate (29). Potassium (490 mg, 0.013 mol) was added into a well stirred solution of **13** (3.0 g, 0.014 mol) in anhydrous tetrahydrofuran (150 mL) and the mixture was refluxed until the metal disappeared. The cooled mixture was treated with 18-crown-6 (3.7 g, 0.014 mol), then a solution of 4-nitrobenzenesulfonyl chloride (3.1 g, 0.014 mol) in anhydrous tetrahydrofuran (250 mL) was dropped into the above mixture over 30 min. After addition the solution was stirred at room temperature for 2.5 h, then the solvent was removed. The residue was treated with water (200 mL) and extracted with ethyl acetate (3×100 mL). The organic extracts were collected, washed with brine and dried. Removal of the solvent gave a residue which was chromatographed on aluminum oxide column (ethyl acetate as eluent) to furnish **29** (2.19 g, 39% yield); IR: ν 1700 (CO) cm^{-1}; ^1H NMR ($CDCl_3$): δ 1.26 (t, 3H, CH_3), 4.23 (q, 2H, CH_2), 7.26 (d, 1H, $J_{2,5}=2.8$ Hz, pyrrole C5-H), 7.33 (m, 2H, pyridine C3-H and C5-H), 7.88 (d, 1H, $J_{2,5}=2.8$ Hz, pyrrole C2-H), 8.16 (m, 2H, benzene C3-H and C5-H), 8.42 (m, 2H, benzene C2-H

Table 4. Chemical and physical data of derivatives **13**–**18** and **25**–**30**

Compd	Formula	Mp (°C)	Recrystallization solvent[a]	Yield (%)	Reaction time (h)	Chromatographic system[b]
13	$C_{12}H_{12}N_2O_2$	134–135	a	99	0.25	—
14	$C_{10}H_{10}N_4O$	270–272	b	73	0.25	—
15	$C_{13}H_{14}N_2O_2$	58–60	c	84	2.5	A
16	$C_{14}H_{16}N_2O_2$	99–100	c	74	2.5	A
17	$C_{14}H_{16}N_2O_2$	199–201	d	36	0.25	A
18	$C_{12}H_{14}N_4O$	257–259	e	12	3	—
25	$C_{19}H_{17}C1N_2O_2$	Oil	—	55	1.5	B
26	$C_{21}H_{22}N_2O_2$	Oil	—	20	1.5	B
27	$C_{17}H_{15}C1N_4O$	165–167	d	33	1	—
28	$C_{19}H_{18}N_2O_4S$	107–108	c	90	1	C
29	$C_{18}H_{15}N_3O_6S$	174–175	a	39	3	A
30	$C_{17}H_{16}N_2O_3S$	135–137	a	69	0.5	—

[a]a, benzene; b, ethanol; c, benzene/cyclohexane; d, toluene; e, isopropanol.
[b]A, aluminum oxide/ethyl acetate; B, silica gel/ethyl acetate; C, aluminum oxide/chloroform.

and C6-H), 8.58 (m, 2H, pyridine C2-H and C6-H); anal. $C_{18}H_{15}N_3O_6S$ (401.39) C, H, N, S.

Compound **28** was obtained with the same procedure; IR: ν 1720 (CO) cm^{-1}; ^1H NMR ($CDCl_3$): δ 1.26 (t, 3H, CH_2CH_3), 2.45 (s, 3H, CH_3), 4.23 (q, 2H, CH_2), 7.23–7.39 (m, 5H, pyrrole C5-H, pyridine C3-H and C5-H and benzene C3-H and C5-H), 7.83–7.88 (m, 3H, pyrrole C2-H and benzene C2-H and C6-H), 8.57 (m, 2H, pyridine C2-H and C6-H); anal. $C_{19}H_{18}N_2O_4S$ (370.42) C, H, N, S.

1-(4-Methylbenzenesulfonyl)-4-(4-pyridinyl)pyrrole-3-methanol (30). A solution of **28** (300 mg, 0.8 mmol) in anhydrous tetrahydrofuran (6 mL) was added by dropping into a well stirred suspension of lithium aluminum hydride (70 mg, 1.8 mmol) in the same solvent (6 mL). After addition the mixture was stirred at room temperature for 30 min and then carefully treated with crushed ice. The inorganic precipitate was removed and the solution was concentrated and shaken with brine, dried and evaporated to give **30** (180 mg, 69% yield); IR: ν 3180 (OH) cm^{-1}; ^1H NMR ($CDCl_3$): δ 2.41 (s, 3H, CH_3), 2.49 (bs, 1H, OH), 4.61 (s, 2H, CH_2), 7.26–7.45 (m, 6H, pyrrole H, pyridine C3-H and C5-H and benzene C3-H and C5-H), 7.80 (m, 2H, benzene C2-H and C6-H), 8.52 (m, 2H, pyridine C2-H and C6-H); anal. $C_{17}H_{16}N_2O_3S$ (328.39) C, H, N, S.

Ethyl 1-(4-chlorobenzyl)-4-(4-pyridinyl)pyrrole-3-carboxylate (25). A solution of 4-chlorobenzyl chloride (740 mg, 4.6 mmol) in dichloromethane (14 mL) was added by dropping into a well stirred mixture of **13** (1.0 g, 4.6 mmol) and tetrabutylammonium hydrogen sulfate (140 mg, 0.4 mmol) in a mixture of dichloromethane (14 mL) and 50% aqueous NaOH (5 mL) cooled at 0 °C. The resulting mixture was stirred at room temperature for 15 h, then diluted with water (50 mL) and extracted with chloroform (3×25 mL). The organic extracts were collected, washed with brine (3×50 mL) and dried. Removal of the solvent gave a residue which was chromatographed on silica gel column (ethyl acetate as eluent) to give pure **25** (860 mg, 55% yield); IR: ν 1700 (CO) cm^{-1}; ^1H NMR ($CDCl_3$): δ 1.26 (t, 3H, CH_3), 4.22 (q, 2H, CH_2CH_3), 5.05 (s, 2H, CH_2), 6.76 (d, 1H, $J = 2.2$ Hz, pyrrole C5-H), 7.11–7.42 (m, 7H, pyrrole C2-H, pyridine C3-H and C5-H and benzene H), 8.53 (m, 2H, pyridine C2-H and C6-H); anal. $C_{19}H_{17}ClN_2O_2$ (340.81) C, H, N, Cl.

By this procedure were prepared compounds **15**, **16** and **26**; their spectroscopic data are reported below.

15: IR: ν 1705 (CO) cm^{-1}; ^1H NMR ($CDCl_3$): δ 1.26 (t, 3H, CH_2CH_3), 3.71 (s, 3H, CH_3), 4.22 (q, 2H, CH_2), 6.74 (d, 1H, $J_{2,5} = 2.5$ Hz, pyrrole C5-H), 7.35 (d, 1H, $J_{2,5} = 2.5$ Hz, pyrrole C2-H), 7.46 (m, 2H, pyridine C3-H and C5-H), 8.53 (m, 2H, pyridine C2-H and C6-H); anal. $C_{13}H_{14}N_2O_2$ (230.27) C, H, N.

16: IR: ν 1705 (CO) cm^{-1}; ^1H NMR ($CDCl_3$): δ 1.27 (t, 3H, OCH_2CH_3), 1.49 (t, 3H, CH_2CH_3), 3.97 (q, 2H, CH_2CH_3), 4.22 (q, 2H, OCH_2CH_3), 6.78 (d, 1H, $J_{2,5} =$ 2.5 Hz, pyrrole C5-H), 7.41–7.44 (m, 3H, pyridine C3-H and C5-H and pyrrole C2-H), 8.53 (m, 2H, pyridine C2-H and C6-H); anal. $C_{14}H_{16}N_2O_2$ (244.29) C, H, N.

26: IR: ν 1700 (CO) cm^{-1}; ^1H NMR ($CDCl_3$): δ 1.00 and 1.19 (2t, 6H, CH_3), 2.46 (q, 2H, CH_2CH_3), 4.12 (q, 2H, OCH_2CH_3), 5.11 (s, 2H, CH_2), 7.08–7.38 (m, 8H, pyridine C3-H and C5-H, pyrrole H and benzene H), 8.57 (m, 2H, pyridine C2-H and C6-H); anal. $C_{21}H_{22}N_2O_2$ (334.42) C, H, N.

4-(4-Pyridinyl)pyrrole-3-carboxyhydrazide (14). A mixture of **13** (500 mg, 2.3 mmol), hydrazine hydrate (3 mL) and ethanol (1.5 mL) was refluxed for 15 min. After cooling the precipitate which formed was filtered and recrystallized from ethanol to obtain pure **14** (340 mg, 73% yield); IR: ν 3280 (NH and NH_2), 1630 (CO) cm^{-1}; ^1H NMR (DMSO-d_6): δ 4.28 (bs, 2H, NH_2), 7.24 (s, 2H, pyrrole H), 7.50 (m, 2H, pyridine C3-H and C5-H), 8.40 (m, 2H, pyridine C2-H and C6-H), 9.08 (bs, 1H, CONH), 11.40 (bs, 1H, NH); anal. $C_{10}H_{10}N_4O$ (202.22) C, H, N.

This procedure was used for the synthesis of derivatives **18** and **27**.

18: IR: ν 3320, 3160 and 3080 (NH and NH_2), 1635 (CO) cm^{-1}; ^1H NMR (DMSO-d_6): δ 1.11 (t, 3H, CH_3), 2.52 (q, 2H, CH_2), 4.25 (bs, 2H, NH_2), 7.18 (m, 3H, pyridine C3-H and C5-H, pyrrole H), 8.44 (m, 2H, pyridine C2-H and C6-H), 8.92 (bs, 1H, CONH), 11.22 (bs, 1H, NH); anal. $C_{12}H_{14}N_4O$ (230.27) C, H, N.

27: IR: ν 3180 (NH and NH_2), 1630 (CO) cm^{-1}; ^1H NMR (DMSO-d_6): δ 4.33 (bs, 2H, NH_2), 5.14 (s, 2H, CH_2), 7.30–7.46 (m, 8H, pyridine C3-H and C5-H, pyrrole H and benzene H), 8.41 (m, 2H, pyridine C2-H and C6-H), 9.16 (bs, 1H, NH); anal. $C_{17}H_{15}ClN_4O$ (326.79) C, H, N, Cl.

Microbiology

Compounds. Test derivatives and drug references were dissolved in DMSO at the initial concentration of 10 mg/mL and stored in cold place until use.

Cytotoxicity. The cytotoxicity of above compounds was tested on VERO cell monolayers (ICN-FLOW), grown in Dulbecco's modified MEM (GIBCO Lab. Inc.) with 2% fetal calf serum. Six-well culture plates were inoculated with 9×10^4 cells. After 24 h the compounds were added and after five further days the cells were detached from wells, trypsinized and counted in a Neubauer chamber. The minimal toxic dose (MTD_{50}) was the concentration of drugs that induced a reduction of 50% of cell growth with respect to the control.

Antimycobacterial activity. All compounds were preliminarily assayed against two freshly isolated clinical strains, *M. fortuitum* CA10 and *M. tuberculosis* B814, according to diffusion method in agar.[33] Growth media were Mueller-Hinton (Difco) containing 10% of OADC (oleic acid, albumin and dextrose complex) for

M. fortuitum and Middlebrook 7H9 agar (Difco) with 10% of ADC (albumin dextrose complex) for *M. tuberculosis*. Substances were tested at the single dose of 100 μg/mL. Compounds that showed activity in the preliminary test were assayed for inhibitory activity against *M. tuberculosis* CIP 103471 in comparison with streptomycin (SM) and isoniazid (INH) as reference drugs. A broth microdilution assay was used for rapidly growing strains.[33–35] Minimum inhibitory concentrations (MICs in μg/mL) for each compound were determined. The MICs for test derivatives and controls were determined by the BACTEC 460 TB method.[36,37]

Acknowledgements

Thanks are due to Ministero della Sanità, Istituto Superiore di Sanità, II Progetto Tubercolosi 1997 (Grant No. 96/D/T48) and to Italian MURST for partial support.

References

1. Baker, R. W.; Mitscher, L. A.; Arain, T. M.; Shawar, R.; Stover, C. K. *Ann. Rep. Med. Chem.* **1996**, *31*, 161.
2. Duncan, K. *Exp. Opin. Ther. Patents* **1997**, *7*, 129.
3. Niccolai, D.; Tarsi, L.; Thomas, R. J. *Chem. Commun.* **1997**, 2333.
4. Horsburgh, C. R., Jr. *The New England Journal of Medicine* **1991**, *324*, 1332.
5. Heifets, L. *Antimicrob. Agents Chemother.* **1996**, *40*, 1759.
6. Barbachyn, M. R.; Hutchinson, D. K.; Brickner, S. J.; Cynamom, M. H.; Kilburn, J. O.; Klemens, S. P.; Glickman, S. E.; Grega, K. C.; Hendges, S. K.; Toops, D. S.; Ford, C. W.; Zurenke, G. E. *J. Med. Chem.* **1996**, *39*, 680.
7. Ashtekar, D. R.; Costa-Pereira, R.; Shrinivasan, T.; Iyyer, R.; Vishvanathan, N.; Rittel, W. *Diagn. Microbiol. Infect. Dis.* **1991**, *14*, 465.
8. Nagarajan, K.; Shankar, R. G.; Rajappa, S.; Shenopy, S. J.; Costa-Pereira, R. *Eur. J. Med. Chem.* **1989**, *24*, 631.
9. Ashtekar, D. R.; Costa-Pereira, R.; Nagarajan, K.; Vishvanathan, N.; Bhatt, A. D.; Rittel, W. *Antimicrob. Agents Chemother.* **1993**, *37*, 183.
10. Cynamon, M. H.; Gimi, R.; Gyenes, F.; Sharpe, C. A.; Bergmann, K. E.; Han, H. J.; Gregor, L. B.; Rapolu, R.; Luciano, G.; Welch, J. T. *J. Med. Chem.* **1995**, *38*, 3902.
11. Cynamon, M. H.; Speirs, R. J.; Welch, J. T. *Antimicrob. Agents Chemother.* **1998**, *42*, 462.
12. Johnsson, K.; Schultz, P. G. *J. Am. Chem. Soc.* **1994**, *116*, 7425.
13. Dessen, A.; Quemard, A.; Blanchard, J. S.; Jacobs, W. R., Jr; Sacchettini, J. C. *Science* **1995**, *24*, 1638.
14. Deidda, D.; Lampis, G.; Fioravanti, R.; Biava, M.; Porretta, G. C.; Zanetti, S.; Pompei, R. *Antimicrob. Agents Chemother.* **1998**, *42*, 3035.
15. Di Santo, R.; Costi, R.; Artico, M.; Massa, S.; Lampis, G.; Deidda, D.; Pompei, R. *Bioorg. Med. Chem. Lett.* **1998**, *8*, 2931.
16. Massa, S.; Di Santo, R.; Mai, A.; Botta, M.; Artico, M.; Panico, S.; Simonetti, G. *Farmaco.* **1990**, *45*, 833.
17. Massa, S.; Di Santo, R.; Costi, R.; Mai, A.; Artico, M.; Retico, A.; Apuzzo, G.; Artico, M.; Simonetti, G. *Med. Chem. Research* **1993**, *3*, 192.
18. Massa, S.; Di Santo, R.; Artico, M.; Costi, R.; Di Filippo, C.; Simonetti, G.; Retico, A.; Artico, M. *Eur. Bull. Drug Research* **1992**, *1*, 12.
19. Cramer, R. D.III; Patterson, D.; Bunce, J. *J. Am. Chem. Soc.* **1988**, *110*, 5959.
20. Cramer, R. D., III; DePriest, S.; Patterson, D.; Hecht, P. In *3-D-QSAR in Drug Design*; Kubinyi, H., Ed.; ESCOM: Leiden, 1993; pp 443–485.
21. Cramer, R. D., III; Wold, S. B. US Patent 5,025,388, 18 June 1991.
22. Hallinan, E. A.; Hagen, T. J.; Husa, R. K.; Tsymbalov, S.; Rao, S. N.; van Hoeck, J.-P.; Rafferty, M. F.; Stapelfeld, A.; Savage, M. A.; Reichman, M. *J. Med. Chem.* **1993**, *36*, 3293.
23. van Leusen, A. M.; Bouma, R. J.; Possel, O. *Tetrahedron Lett.* **1975**, 3487.
24. Greco, G.; Novellino, E.; Fiorini, I.; Nacci, V.; Campiani, G.; Ciani, S. M.; Garofalo, A.; Bernasconi, P.; Mennini, T. *J. Med. Chem.* **1994**, *37*, 4100.
25. Tafi, A.; Anastassopoulous, J.; Theophanides, T.; Botta, M.; Corelli, F.; Massa, S.; Artico, M.; Costi, R.; Di Santo, R.; Ragno, R. *J. Med. Chem.* **1996**, *39*, 1227.
26. In Tripos Associates, Inc., 1699 S Hanley Rd, St. Louis, MO 63144, USA.
27. Halgren, T. A. *Journal of Computational Chemistry* **1996**, *17*, 490.
28. Lindgren, F.; Geladi, P.; Rannar, S.; Wold, S. *J. Chemometrics* **1994**, *8*, 349.
29. Clark, M.; Cramer, R. I. *Quant. Struct. Act. Relat.* **1993**, *12*, 137.
30. In Kellogg, K. E.; Abraham, D. J.; Richmond, VA 23298–0540.
31. Kellog, G.; Semus, S.; Abraham, D. *HINT: J. Comput. Aided Mol. Design* **1991**, *5*, 545.
32. Cramer, C. J. *Acc. Chem. Res.* **1993**, *26*, 599.
33. Hawkins, J. E.; Wallace, R. J.; Brown, B. A. In *Manual of Clinical Microbiology*; Balows, W. J.; Hausler, K. L.; Hermann, K. L.; Isemberg, H. D.; Shadomy, H. J., Eds. ASM: Washington, DC, 1991; pp 1138–1152.
34. National Committee for Clinical Laboratory Standards. *Antimycobacterial Susceptibility Testing*. Proposed Standard M24; NCCLS: Villanova, PA, 1990.
35. Brown, B. A.; Swenson, J. M.; Wallace, R. J., Jr. In *Clinical Microbiology Procedures Handbook* American Society for Microbiology: Washington, DC, 1992; Vol. I.
36. Helfets, L. *Antimicrob. Agents Chemother.* **1996**, *40*, 1759.
37. Inderlied, C. B.; Salenger, M. In *Manual of Clinical Microbiology*, 5th ed.; Murray, P. R.; Baron, E. J.; Pfaller, M. A.; Tenover, F. C.; Volken, R. H., Eds.; American Society of Microbiology: Washington, DC; pp 1385–1404.